

# A compact 2D finite-difference time-domain method for full-vectorial analyses of photonic crystal fibers with material dispersion

JUAN JUAN HU\*, PING SHUM, GUOBIN REN

Network Technology Research Centre, Nanyang Technological University, 50 Nanyang Drive, Research Techno Plaza, Singapore – 637553

We present a compact 2D finite-difference time-domain full-vectorial method by reformulating the time dependent Maxwell's curl equations with electric flux density and magnetic field intensity, with auxiliary differential equations using complex-conjugate pole-residue pairs. The model is general and robust to treat general frequency-dependent material and it can be easily extended for nonlinearity analysis. As an example, the Sellmeier equation is implicitly incorporated as a special case of the general formulation to account for material dispersion of fused silica. The correlation results match well with multipole method. The relative error is within 0.02%.

(Received May 18, 2007; accepted June 27, 2007)

*Keywords:* Finite-difference time-domain (FDTD), Photonic crystal fibers (PCF), Material dispersion, Auxiliary differential equation (ADE)

## 1. Introduction

Photonic crystal fibers (PCFs) have attracted a great deal of attention in optics research domain since its introduction in 1996[1]. PCFs, generally classified in two classes, i.e. index-guiding PCF and photonic bandgap PCF, can offer many superior properties over conventional step-index fibers, such as endlessly single-mode operation[2], high birefringence[3], high/low nonlinearity[4], tailorable dispersion[5], or even guidance in a hollow core[6]. With the growing interest in PCFs, effective numerical modeling is an indispensable tool as mathematical analyses are difficult for PCF. Several modeling methods have been proposed to study the modal properties of PCFs, including the multipole method[7,8], the beam propagation method[9], the finite element method[10], and the finite-difference method in time domain (FDTD)[11] or frequency domain (FDFD)[12]. Among all these methods, the FDTD method has been recognized as a powerful technique.

A compact two-dimensional FDTD (C2D-FDTD) approach is proposed to solve guided modes in PCF by assuming the propagation constant real and constant along fiber axis[13]. Recently W. Jiang *et al.* [14] proposed that by implicitly including Sellmeier formula in the formulation by introducing an auxiliary polarization current density, material dispersion of fused silica can be processed. However, for other frequency dependent material, which Sellmeier formula may not provide accurate estimation of the material permittivity, their formulation is no longer sufficient. To give a general and comprehensive modeling for material dispersion in PCF, we use a generalized formulation of Maxwell's curl equations by flux density and magnetic field with complex-conjugate pole-residue pairs, and we demonstrate

that our approach is more general and robust to treat complicated frequency dependent material in PCF. The effective indices of guided modes are calculated by our FDTD model are found to be within 0.02% relative error compared to multipole method.

## 2. Formulation

For a linear isotropic material in a source-free region, the time-dependent Maxwell's curls equations can be written using the flux density in a form:

$$\frac{\partial \tilde{\mathbf{D}}}{\partial t} = \frac{1}{\sqrt{\epsilon_0 \mu_0}} \nabla \times \mathbf{H} \quad (1)$$

$$\tilde{\mathbf{D}}(\omega) = \epsilon_r^*(\omega) \cdot \tilde{\mathbf{E}}(\omega) \quad (2)$$

$$\frac{\partial \mathbf{H}}{\partial t} = -\frac{1}{\sqrt{\epsilon_0 \mu_0}} \nabla \times \tilde{\mathbf{E}} \quad (3)$$

where  $\tilde{\mathbf{E}} = \sqrt{\frac{\epsilon_0}{\mu_0}} \cdot \mathbf{E}$  and  $\tilde{\mathbf{D}} = \sqrt{\frac{1}{\epsilon_0 \mu_0}} \cdot \mathbf{D}$ ,  $\epsilon_r^*(\omega)$

characterizes the material constitution between electric field intensity and electric flux density, and it is in frequency domain. The advantage of using electric flux density and magnetic field intensity formulation comes when we deal with complicate materials, such as frequency-dependent material, lossy or gain medium material[15] etc, as we can see the complexity only adds to the constitutive equation which leaves the other two curl equations unaffected. Generally, a comprehensive

expression for  $\varepsilon_r^*(\omega)$  should comprise several terms accounting for the linear index of the system, material dispersion or frequency dependence on the material index, and nonlinearities as a function of intensity. For general dispersive material, we start from a general permittivity formula as the sum of complex-conjugate pole-residue pairs [16] for a given dispersive medium. We can add the conductivity of the material into consideration without adding much complexity. The last term in Eq. (4) denotes Kerr-type nonlinearity.

$$\varepsilon_r(\omega) = \varepsilon_\infty + \sum_{k=1}^K c_k / (j\omega - \alpha_k) + c_k^* / (j\omega - \alpha_k^*) + \frac{\sigma}{j\omega\varepsilon_0} + \rho |E|^2 \quad (4)$$

In this paper, we discuss the dispersive material modeling in linear regime. The constitution equation can be expanded as

$$\tilde{\mathbf{D}}(\omega) = \varepsilon_\infty \tilde{\mathbf{E}}(\omega) + \sum_{k=1}^K c_k / (j\omega - \alpha_k) + c_k^* / (j\omega - \alpha_k^*) \cdot \tilde{\mathbf{E}}(\omega) + \frac{\sigma}{j\omega\varepsilon_0} \cdot \tilde{\mathbf{E}}(\omega) \quad (5)$$

Here we define the auxiliary parameter  $S$  and  $S^*$  pairs to describe the material dispersion and  $I$  to describe the conductivity term. In the sampled time domain, at every time step  $n$ , the parameters  $S_k$ ,  $I$  and electrical field are updated accordingly.

$$S_k^n = \frac{\Delta t c_k}{1 - \Delta t \alpha_k} \tilde{\mathbf{E}}^n + \frac{1}{1 - \Delta t \alpha_k} S_k^{n-1} \quad (6)$$

$$I^n = I^{n-1} + \frac{\sigma \cdot \Delta t}{\varepsilon_0} \tilde{\mathbf{E}}^n \quad (7)$$

It should be noted that everything concerning the medium is contained in Eq (4), the calculation of the flux density and magnetic field which contains spatial derivatives are unchanged with respect to media. In the following sections, we use  $D$ ,  $E$  and  $H$  to denote the normalized components.

For the guided modes in PCF, C2D-FDTD method explicitly factors out the time-dependence of  $\exp(-j\beta z)$  where  $z$  is the propagation direction along the fiber axis. The unit cell of the two-dimensional FDTD mesh across the fiber transverse plane is depicted in Fig. 1. The complete set of equations for field components as well as auxiliary differential equations is obtained as Eqs. (8) to (23).

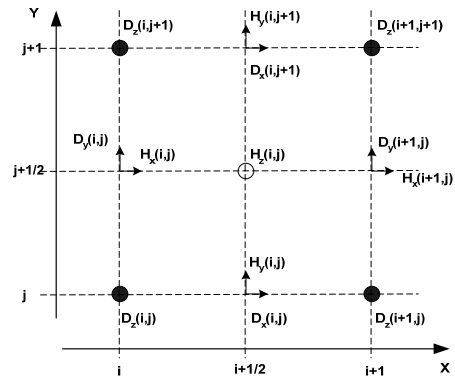


Fig. 1. Unit cell of the two-dimensional FDTD mesh.

$$D_x |_{i+1/2,j}^{n+1/2} = D_x |_{i+1/2,j}^{n-1/2} + \frac{\Delta t}{\sqrt{\varepsilon_0 \mu_0}} \left( \frac{H_z |_{i+1/2,j+1/2}^n - H_z |_{i+1/2,j-1/2}^n}{\Delta y} + j\beta H_y |_{i+1/2,j}^n \right) \quad (8)$$

$$D_y |_{i,j+1/2}^{n+1/2} = D_y |_{i,j+1/2}^{n-1/2} + \frac{\Delta t}{\sqrt{\varepsilon_0 \mu_0}} \left( -\frac{H_z |_{i+1/2,j+1/2}^n - H_z |_{i-1/2,j+1/2}^n}{\Delta x} - j\beta H_x |_{i,j+1/2}^n \right) \quad (9)$$

$$D_z |_{i,j}^{n+1/2} = D_z |_{i,j}^{n-1/2} + \frac{\Delta t}{\sqrt{\varepsilon_0 \mu_0}} \left( \frac{H_y |_{i+1/2,j}^n - H_y |_{i-1/2,j}^n}{\Delta x} - \frac{H_x |_{i,j+1/2}^n - H_x |_{i,j-1/2}^n}{\Delta y} \right) \quad (10)$$

$$E_x |_{i+1/2,j}^{n+1/2} = \frac{D_x |_{i+1/2,j}^{n+1/2} - I_x |_{i+1/2,j}^{n-1/2} - 2 \sum_{k=1}^K \text{Re}(\kappa_k |_{i+1/2,j} S_{k,x} |_{i+1/2,j}^{n-1/2})}{\varepsilon_\infty + \frac{\sigma |_{i+1/2,j} \cdot \Delta t}{\varepsilon_0} + 2 \sum_{k=1}^K \text{Re}(\nu_k |_{i+1/2,j})} \quad (11)$$

$$S_{k,x} |_{i+1/2,j}^{n+1/2} = \kappa_k |_{i+1/2,j} S_{k,x} |_{i+1/2,j}^{n-1/2} + \nu_k |_{i+1/2,j} E_x |_{i+1/2,j}^{n-1/2} \quad (12)$$

$$I_x |_{i+1/2,j}^{n+1/2} = I_x |_{i+1/2,j}^{n-1/2} + \frac{\sigma |_{i+1/2,j} \cdot \Delta t}{\varepsilon_0} \cdot E_x |_{i+1/2,j}^{n+1/2} \quad (13)$$

$$E_y |_{i,j+1/2}^{n+1/2} = \frac{D_y |_{i,j+1/2}^{n+1/2} - I_y |_{i,j+1/2}^{n-1/2} - 2 \sum_{k=1}^K \text{Re}(\kappa_k |_{i,j+1/2} S_{k,y} |_{i,j+1/2}^{n-1/2})}{\varepsilon_\infty + \frac{\sigma |_{i,j+1/2} \cdot \Delta t}{\varepsilon_0} + 2 \sum_{k=1}^K \text{Re}(\nu_k |_{i,j+1/2})} \quad (14)$$

$$S_{k,y} |_{i,j+1/2}^{n+1/2} = \kappa_k |_{i,j+1/2} S_{k,y} |_{i,j+1/2}^{n-1/2} + \nu_k |_{i,j+1/2} E_y |_{i,j+1/2}^{n-1/2} \quad (15)$$

$$I_y |_{i,j+1/2}^{n+1/2} = I_y |_{i,j+1/2}^{n-1/2} + \frac{\sigma |_{i,j+1/2} \cdot \Delta t}{\varepsilon_0} \cdot E_y |_{i,j+1/2}^{n+1/2} \quad (16)$$

$$E_z |_{i,j}^{n+1/2} = \frac{D_z |_{i,j}^{n+1/2} - I_z |_{i,j}^{n-1/2} - 2 \sum_{k=1}^K \text{Re}(\kappa_k |_{i,j} S_{k,z} |_{i,j}^{n-1/2})}{\varepsilon_\infty + \frac{\sigma |_{i,j} \cdot \Delta t}{\varepsilon_0} + 2 \sum_{k=1}^K \text{Re}(\nu_k |_{i,j})} \quad (17)$$

$$S_{k,z} |_{i,j}^{n+1/2} = \kappa_k |_{i,j} S_{k,z} |_{i,j}^{n-1/2} + \nu_k |_{i,j} E_z |_{i,j}^{n-1/2} \quad (18)$$

$$I_z |_{i,j}^{n+1/2} = I_z |_{i,j}^{n-1/2} + \frac{\sigma |_{i,j} \cdot \Delta t}{\varepsilon_0} \cdot E_z |_{i,j}^{n+1/2} \quad (19)$$

$$H_x |_{i,j+1/2}^{n+1} = H_x |_{i,j+1/2}^n + \frac{\Delta t}{\sqrt{\varepsilon_0 \mu_0}} \left( -\frac{E_z |_{i,j+1/2}^{n+1/2} - E_z |_{i,j}^{n+1/2}}{\Delta y} \right)$$

$$H_y|_{i+1/2,j}^{n+1} = H_y|_{i+1/2,j}^n + \frac{\Delta t}{\sqrt{\epsilon_0\mu_0}} \left( \frac{-j\beta E_y|_{i,j}^{n+1/2}}{\Delta x} + \frac{E_z|_{i+1,j}^{n+1/2} - E_z|_{i,j}^{n+1/2}}{\Delta x} \right) \quad (20)$$

$$H_z|_{i+1/2,j+1/2}^{n+1} = H_z|_{i+1/2,j+1/2}^n + \frac{\Delta t}{\sqrt{\epsilon_0\mu_0}} \left( \frac{E_x|_{i+1/2,j+1}^{n+1/2} - E_x|_{i+1/2,j}^{n+1/2}}{\Delta y} + \frac{E_y|_{i+1,j+1/2}^{n+1/2} - E_y|_{i,j+1/2}^{n+1/2}}{\Delta x} \right) \quad (22)$$

$$\text{where } \kappa_k = \frac{1 + \alpha_k \Delta t / 2}{1 + \alpha_k \Delta t / 2}, \nu_k = \frac{c_k \Delta t}{1 - \alpha_k \Delta t / 2} \quad (23)$$

The index  $n$  denotes the discrete time step, indexes  $I$  and  $j$  denote the discretized grid point in the  $x$ - $y$  plane respectively.  $\Delta t$  is the time increment, and  $\Delta x$  and  $\Delta y$  are the grid size along  $x$ - and  $y$ -directions, respectively. The parameters  $\kappa_k$  and  $\nu_k$  are calculated using Eq. (23) and they are generally complex numbers,  $\alpha_k$  and  $c_k$  are position dependent parameters which are corresponding to different materials.

The above presented formulation is able to treat Debye media and Lorentz media in an unified manner [16], which definitely reduces implementation cost when dealing with different frequency-dependent materials. The Sellmeier formula is a special case of this model. In particular, let  $\epsilon_\infty = 1$ ,  $c_k = j b_k \omega_k / 2$  and  $\alpha_k = j \omega_k$ , the above formulation is exactly the same as ADE formulation for a medium modeled by Sellmeier equation.

$$\epsilon_r(\omega) = 1 + \sum_{k=1}^3 \frac{b_k \omega_k^2}{\omega_k^2 - \omega^2} \quad (24)$$

For bulk fused silica,  $b_1=0.6961663$ ,  $b_2=0.4079426$ ,  $b_3=0.8974794$ ,  $\lambda_{1j}=0.0684043 \mu\text{m}$ ,  $\lambda_{2j}=0.1162414 \mu\text{m}$ ,

$\lambda_{3j}=9.896161 \mu\text{m}$ , where  $\lambda_j=2\pi c/\omega_j$  and  $c$  is velocity of light in vacuum.  $c_k$  and  $\alpha_k$  are calculated accordingly and position dependent parameters  $\kappa_k$  and  $\nu_k$  are known. Averaging techniques in the sampling is applied to improve the accuracy and convergence of the FDTD algorithm. To simulate the unbounded regions, we use perfectly matched layer (PML) method to allow the incoming wave to pass through the boundary with minimized reflection. An artificial initial field distribution is introduced and sufficient time steps are used to absorb unphysical field components with only guided modes remain. The calculated fields are then transformed into frequency domain to extract spectral information.

### 3. Numerical results

Let consider a structure with a single ring of six equally spaced air holes with  $d = 5 \mu\text{m}$ ,  $\Lambda = 6.75\mu\text{m}$ ,  $\lambda = 1.43 \mu\text{m}$ , the background material is silica. The

dielectric constant is described by Sellmeier formula, and the conductivity is 0.  $d$  denotes the air hole diameter,  $\Lambda$  is the hole to hole distance. The computation domain is shown in Fig.2 with six holes in the cladding, fiber core is solid. A total of 19600 ( $140 \times 140$ ) mesh points are in the computation domain, and the total number of the time steps is 100,000, with each time step

$\Delta t = 0.1 / c \sqrt{\Delta x^{-2} + \Delta y^{-2} + (\beta/2)^2}$ . The effective index calculated by the current FDTD program is 1.441469, compared to multipole method [8] which is 1.441465, we see a very good agreement. We further investigate the mode profile of  $x$ -polarization at this wavelength as shown in Fig. 2, which are normalized electrical fields and they correlate with multipole method very well. In our FDTD program, the propagation constant  $\beta$  is the independent variable rather than the free space wavelength  $\lambda$ . To correlate the results with multipole method which uses wavelength as the input, we performed a *regula falsi* search on the propagation to obtain the desired wavelength before calculating the mode profile.

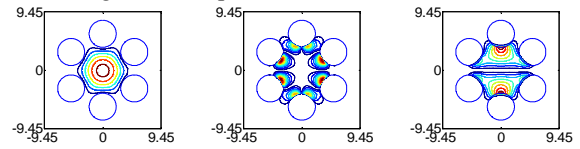


Fig. 2. Normalized fields  $|E_x|$ ,  $|E_y|$ , and  $|E_z|$  for a  $x$ -polarized fundamental mode for a six-hole PCF, with effective mode index  $n_{\text{eff}} = 1.441469$ .

The calculated effective indices of guided modes in the fiber are shown in Fig. 3, which includes the material dispersion. The wavelength spans from  $1.4 \mu\text{m}$  to  $1.5 \mu\text{m}$ , we see that they agree well, the largest relative discrepancy is less than 0.02% from multipole method.

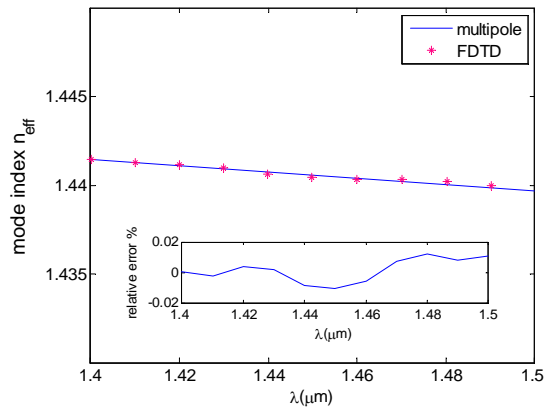


Fig. 3. Mode indices of guided modes of the six-ring photonic crystal fiber. The solid line is obtained by current FDTD model, the dotted line is obtained by multipole method. The largest relative error in effective index is less than 0.02%.

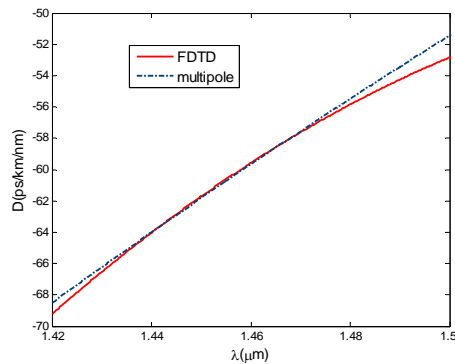


Fig. 4. Total chromatic dispersion of the six-ring photonic crystal fiber. The solid line is obtained by current FDTD model, the dotted line is obtained by multipole method.

The total chromatic dispersion is also calculated and shown in Fig. 4. We could see the results obtained by our FDTD model match well with multipole method. For other materials in PCF, such as nonlinear dispersive materials, or gain mediums, only the constitutive material equation which relates the electric field and flux density needs corresponding modifications. The curl equations concerning flux density and magnetic field remain unchanged.

#### 4. Conclusions

We have given the basic formulation of our FDTD method based on flux density and magnetic field. And we have shown this method is a general approach to calculate the modal properties in PCFs with different frequency-dependent material. With appropriate parameters defined in the complex-conjugate pole-residue poles, general dispersive media can be processed. Fused silica is a special case and Sellmeier formula can be treated as a particular case in the formulation as well. The results are in good correlation with multipole methods. At this stage, lossy medium with position dependent conductivity, as well as material dispersion for general dispersive media can be processed easily in the frame of the model. The method can be extended with nonlinear medium which would require a modification in the constitutive equation only.

#### Acknowledgment

This work was supported in part by the Agency for Science, Technology and Research (A\*STAR), Singapore. The author would like to thank Dr Min Qiu for helpful discussions.

#### References

- [1] J. C. Knight, T. A. Birks, P. St. J. Russell, D. M. Atkin, *Opt. Lett.* **21**, 1547 (1996).
- [2] P. St. J. Russell, *Science* **299**, 358 (2003).
- [3] T. P. Hansen, J. Broeng, S.E.B. Libori, E. Knudsen, A. Bjarklev, J.R. Jensen, and H. Simonsen, *IEEE Photon. Technol. Lett.* **13**, 588 (2001).
- [4] R. Hainberger, S. Watanabe, *IEEE Photon. Technol. Lett.* **17**, 70 (2005).
- [5] K. Saitoh, M. Koshiba. *Optics Express* **12**, 2027 (2004).
- [6] M. Yan, P. Shum, X. Yu, *IEEE Photon. Technol. Lett.* **17**, 1438 (2005).
- [7] T. P. White, B. T. Kuhlmeiy, R. C. McPhedran, D. Maystre, G. Renversez, C. Martijin de Sterke, L. C. Botten, *J. Opt. Soc. Am. B*, **19**, 2322 (2002).
- [8] B. T. Kuhlmeiy, T. P. White, G. Renversez, D. Maystre, L. C. Botten, C. Martijin de Sterke, R. C. McPhedran, *J. Opt. Soc. Am. B* **19**, 2331 (2002).
- [9] R. Scarmozzino, A. Gopinath, R. Pregla, S. Helfert, *J. Selected Topics in Quantum Electronics* **6**, 150 (2000).
- [10] F. Brechet, J. Marcon, D. Pagnoux, P. Roy, *Opt. Fiber Technol.* **6**, 181 (2000).
- [11] A. Taflove, Artech House, Norwood, MA, 1995.
- [12] S. Guo, F. Wu, S. Albin, H. Tai and R.S. Rogowski, *Opt. Express* **12**, 3341 (2004).
- [13] M. Qiu, *Microw. Opt. Technol. Lett.* **30**, 327 (2001).
- [14] W. Jiang, *J. Lightw. Technol.* **24**, 4417 (2006).
- [15] D. M. Sullivan, *IEEE Microwave Theory and Techniques Society*, 2000.
- [16] M. Han, R. W. Dutton, S. Fan, *IEEE Microw. Wireless Compon. Lett.*, **16**, 2006.

\*Corresponding author: hujuanjuan@pmail.ntu.edu.sg